Achieving Extreme Light Intensities using Optically Curved Relativistic Plasma Mirrors

Henri Vincenti

Phys. Rev. Lett. **123**, 105001 — Published 3 September 2019

DOI: 10.1103/PhysRevLett.123.105001

Achieving extreme light intensities using optically-curved relativistic plasma mirrors

Henri Vincenti[1, *]

[1] *LIDYL, CEA, CNRS, Université Paris-Saclay, CEA Saclay, 91 191 Gif-sur-Yvette, France*

(Dated: August 2, 2019)

This letter proposes a realistic implementation of the Curved Relativistic Mirror concept to reach unprecedented light intensities in experiments. The scheme is based on relativistic plasma mirrors that are optically-curved by laser radiation pressure. Its validity is supported by cutting-edge 3D Particle-In-Cell simulations and a theoretical model, which show that intensities above $10^{25} W.cm^{-2}$ could be reached with a 3PW laser. Its very high robustness to laser and plasma imperfections is shown to surpass all previous schemes and should enable its implementation on existing PW laser facilities.

PACS numbers: Valid PACS appear here

The advent of high-power ultra-short lasers [1] has triggered the quest for novel schemes that would allow reaching intensities above $10^{25} W.cm^{-2}$ or even up to the Schwinger limit $10^{29} W.cm^{-2}$. Such intensities would give access to unexplored strong field Quantum Electrodynamics (QED) regimes [2, 3], where e-/e+ cascades are produced from single electrons [4] and vacuum is ripped apart [5–7]. Yet, these light intensities are still more than three orders of magnitude higher than the ones delivered by current PetaWatt (PW) laser technology [8, 9], hence calling for the design of novel solutions.

So far, scientists have relied on the design of experiments involving head-on collisions between GeV-class electron beams and high intensity lasers [10–12], in which the field experienced by electrons in their rest frame can approach or even exceed the Schwinger field.

Another very promising complementary path to reach extreme intensities is the Curved Relativistic Mirror (CRM) concept, which consists in reflecting a laser from a CRM to induce: (i) a temporal compression and Doppler frequency upshift of the incident light and (ii) a focusing of the Doppler upshifted laser light to a tinier spot than the one possible with the incident laser frequency. Since its emergence in 1952 [13] (and complete formulation in 2003 [14]), different implementations of the CRM concept have been proposed [14–17] but none of these has yet led to a detailed and feasible experimental proposal, mainly because: (i) the computational tools/resources available so far were insufficient to numerically validate and study implementations of this concept (ii) they are experimentally unrealistic due to their poor robustness to experimental defects [18] or require experimental know-how far beyond the current state-of-the-art. This has considerably hindered the development of the CRM concept in the last decade. In this context, the key challenge to solve is to design a novel scheme enabling experimental implementation of the CRM concept.

In this letter, I propose a realistic all-optical scheme based on so-called 'plasma mirrors' [19, 20] (abbreviated PM), which is highly robust to experimental imperfections and would allow reaching intensities above $10^{25} W.cm^{-2}$ with PW lasers being brought into operations worldwide. The general principle of this scheme is sketched on Fig. 1 (a) and detailed below.

PMs are formed when a high power femtosecond laser with high contrast (red) is focused on an initially flat solid target. At focus, the intense laser field quasi-instantly ionizes matter and creates a dense plasma (gray scale) that specularly reflects the incident light. Upon reflection on this PM, the laser field drives relativistic oscillations of the PM surface that induce a periodic temporal compression [16, 21, 22] of the reflected field through the Doppler effect. This periodic modulation produces a high-harmonic spectrum in the frequency domain [23–25], associated to a train of attosecond pulses in the time domain (after filtering the incident laser frequency). At focus, the spatially-varying laser intensity (for gaussian beams) is responsible for a curvature of the PM surface by radiation pressure associated to a PM denting parameter δ_p at the center of the laser focal spot (cf. Fig. 1 (a)). Several studies have shown that this optically-curved surface can in turn focus the high order Doppler harmonic beams (purple) [26, 27]. Yet, these studies [28, 29] have considerably underestimated the achievable intensity gains, some reporting $\times 2$ intensity gains only with multi-PW lasers [29]. As a consequence, radiation pressure has not been envisaged to reach extreme light intensification so far.

In this paper, it is instead shown that for realistic and experimentally achievable laser-plasma conditions, harmonic focusing by radiation pressure constitutes a feasible implementation of the CRM concept, which can lead to huge light intensification by up to 3 orders of magnitude at PM focus.

Three-dimensional (3D) Particle-In-Cell (PIC) simulations of the interaction of a PM with at PW laser (under optimal physical conditions to be explained thereafter) were used to bring unambiguous evidence of the validity of this scheme. Such simulations are extremely challenging and could not be performed so far with standard PIC codes due to the lack of accuracy of the finite difference Maxwell solver [30, 31]. Thanks to the recent

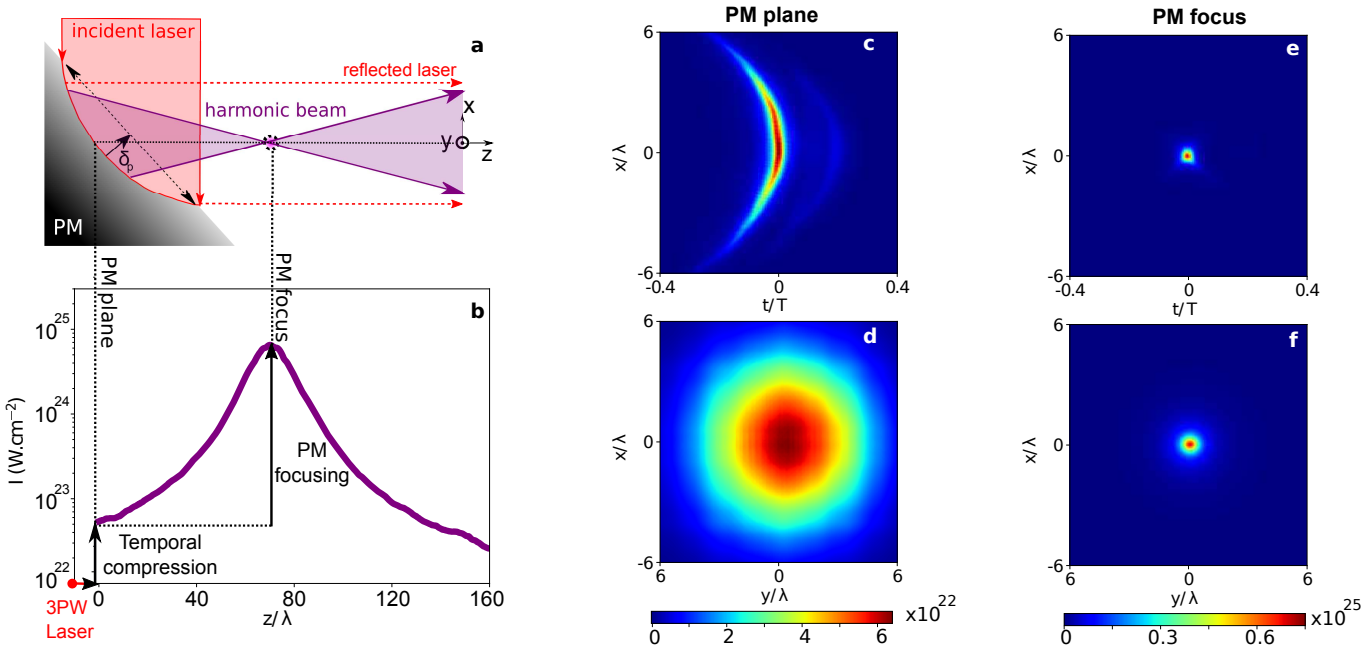

FIG. 1. 3D PIC simulation of PM focusing for optimal parameters $\theta = 45^o$, $L = \lambda_L/8$ and normalized laser amplitude $a_0 = 75$. (a) sketch of the laser-PM interaction (b) Reflected field intensity vs distance z to the PM. (c) and (e) respectively show one optical laser cycle only of the spatio-temporal intensity profile $I(x,t)$ of the reflected field at PM plane and PM focus. (d) and (f) respectively show the reflected beam spatial intensity profile $I(x,y)$ at PM plane and PM focus. On (c-f) the color scale represents light intensity in units of $W.cm^{-2}$.

development and optimization of novel massively parallel and highly accurate pseudo-spectral Maxwell solvers in the PIC code WARP+PICSAR [31–37], it was recently demonstrated that these 3D simulations can now be addressed on the largest supercomputers. In the following are presented results from a 3D PIC simulation of PMs performed with this code on the MIRA cluster at the Argonne Leadership Computer Facility (ALCF). The simulation required the full MIRA machine ($\approx$ 0.8 million cores) during 24 hours i.e a total of $\approx$ 20 millions core hours. As opposed to other proposed schemes [15, 16] where such 3D 'first principles' validations are still missing, this work provides the first accurate 3D PIC modelling of Doppler harmonic generation and focusing by PMs.

The 3D simulation considered a 3PW laser of $60J$ energy and $\approx$ $20fs$ duration with intensity $I \approx 1.2 \times 10^{22} W.cm^{-2}$ (laser normalized amplitude $a_0 = 0.85\sqrt{I[10^{18}W.cm^{-2}]}\lambda[\mu m] \approx 75$ for a laser wavelength $\lambda = 0.8\mu m$) obliquely incident with an angle $\theta = 45^o$ on a PM. The laser waist is $w_L = 5\lambda$. The PM is assumed to have an exponential pre-plasma of gradient scale length $L = \lambda/8$ that can be formed in experiments by sending a pre-pulse beam with an adjustable delay before arrival of the main pulse. The simulation box spans $\approx 4000^3$ cells with a spatial mesh size of $\Delta \approx \lambda/200$ in all directions and a time step $\Delta t \approx T/200$ where T is the laser period. 2 pseudo-particles per cell were used (see Supplemental Material sections 1-2 (SM1-2) [38] for detailed simulation parameters).

Simulation results are displayed on panels (b-f) of Fig. 1. Panel (b) shows that intensities close to $\approx 10^{25} W.cm^{-2}$ are attained at PM focus located at a position $z \approx 72\lambda$ along the specular reflection direction z. This intensification is first due to the periodic temporal Doppler compression of the incident laser within each laser optical cycle, just after its reflection on the relativistic oscillating PM at $z = 0$. Near the laser pulse maximum, this effect leads to the generation of attosecond pulses of 100 as duration (FWHM intensity) carrying an energy of 1.5J. This results in a factor $\approx \times 5$ intensity gain and is clearly visible on panel (c) showing the spatio-temporal intensity map of the reflected field in the PM plane over one laser optical cycle only. Besides temporal compression, the effect of PM curvature on the reflected field can be clearly observed on panel (c) showing a strong curvature of reflected field wavefronts just after reflection at $z = 0$. After a propagation of the reflected field over $\approx 72\lambda$, panels (e) and (f) show a strong spatial compression of the reflected beam profile at PM focus down to 0.4λ in the transverse directions x and y (FWHM intensity). Panel (b) shows that this additional spatial compression yields two additional orders of magnitude increase in intensity.

One can notice that PM focusing is highly efficient and without any major optical aberrations. This can be

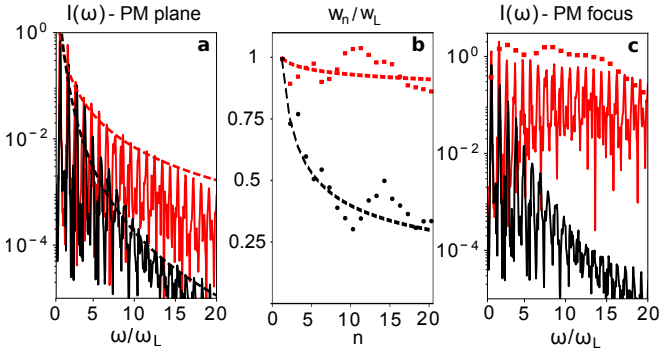

FIG. 2. Effect of PM focusing on harmonic spectra. In all plots, red lines correspond to simulation results obtained for a 3PW incident laser ($a_0 = 75$). The black lines correspond results obtained for a 100 TW laser case ($a_0 = 2$). In all cases, $L = \lambda/8$ was used. (a) Harmonic spectra of the reflected field in the plane of the PM obtained from 2 PIC simulations. (b) Source sizes of harmonic beams obtained from 2D PIC simulations. (c) Harmonic spectra at PM focus deduced from panel (a) using equation (4) and $\delta_p = \lambda/8$. Red squares are harmonic peak maxima obtained from the 3D simulation of Fig. 1.

explained by the parabolic mirror shape of the PM surface obtained with this scheme. Indeed, it was shown in [27] that assuming an exponential density profile of scale length L, the PM denting $\delta(s)$ induced by radiation pressure at position s along the PM surface can be written as $\delta(s) \propto L \ln a(s)$ provided that $a(s) \gg 1$, where $a(s)$ is the spatial amplitude profile of the incident laser. For a gaussian laser beam $a(s) \propto e^{-s^2/w_L^2}$, the PM surface has thus a parabolic shape $\delta(s) \propto s^2$. Furthermore, it can be noticed that despite oblique reflection on the curved PM in the (x, z) plane, no astigmatism affects the reflected field. This should indeed shorten the PM focal length f_p by $\cos\theta$ in this plane compared to the (y, z) plane. Yet, the oblique incidence is also responsible for the formation of an elliptical PM by radiation pressure, which has a focal f_p longer by $1/\cos\theta$ in the (x, z) plane. This eventually gives the same focal length in the (x, z) and (y, z) planes and a perfectly symmetric reflected beam at PM focus as seen on Fig. 1 (f).

The high intensity gains obtained with the proposed scheme, via 3D simulation, are now explained quantitatively. To this end, I first derive a general model of harmonic focusing that gives the harmonic intensity gain after focusing by the PM. Results of this model are then discussed in various physical conditions using more tractable 2D PIC simulations.

In the following, PM is assumed to have a parabolic shape with a denting δ_p at the center of the laser focal spot, as defined on Fig. 1 (a). This curved PM focuses each harmonic beam at a distance $z = z_n$, thus increasing harmonic intensity as follows:

$$I_n^f = I_n^0 \gamma_n^2 \tag{1}$$

where I_n^f is the harmonic intensity at $z = z_n$, I_n^0 is the harmonic intensity at $z = 0$ and $\gamma_n > 1$ is the demagnification factor for harmonic order n. Assuming gaussian harmonics beams, the expression of γ_n can be obtained as detailed in [27]:

$$\gamma_n = \sqrt{1 + \Psi_n^2} \tag{2}$$

where Ψ_n is the PM dimensionless parameter defined as :

$$\Psi_n = \frac{2\pi}{\cos\theta} \left(\frac{w_n}{w_L}\right)^2 \frac{\delta_p}{\lambda_n} \tag{3}$$

with $\lambda_n = \lambda/n$ the harmonic wavelength and w_n the harmonic source size in the PM plane. When the PM denting is much smaller than the harmonic wavelength and/or harmonic beams are generated over a too small part of the laser waist to experience the PM curvature, the PM surface does not focus harmonic beams (i.e. $\Psi_n \ll 1$, $\gamma_n \approx 1$). However, in the opposite case (i.e. $\Psi_n \gg 1$, $\gamma_n \gg 1$), harmonics get focused by the PM and all harmonic orders n are focused at the very same location $z_n = f_p \cos\theta$, where $f_p = w_L^2/2\delta_p$ is the focal length of the PM. In this case the harmonic intensity gain at PM focus writes:

$$\Gamma_n = \frac{I_n^f}{I_n^0} \approx \frac{4\pi^2}{\cos^2\theta} \left(\frac{w_n}{w_L}\right)^2 \left(\frac{\delta_p}{\lambda}\right)^2 n^2 \tag{4}$$

Using equation (4) and knowing the complex spectrum E_n^0 in PM plane (such that $I_n^0 = |E_n^0|^2$), the total theoretical intensity gain Γ at PM focus for the reflected field (composed of all harmonic orders) can be computed numerically from Γ_n (see SM3 [38]).

Assuming a spectrum roll-off factor α defined as $I_n^0 = I_0/n^\alpha$, equation (4) shows that one can get a harmonic intensity increasing with harmonic order n at PM focus, provided that: (i) the harmonic spectrum in PM plane I_n^0 is slowly decaying with n (i.e. $\alpha \leqslant 2$) and (ii) most harmonics are efficiently generated over the laser waist (i.e. $w_n/w_L \approx 1$, independent of n). The increase of harmonic intensity with n originates from a tight focusing of high harmonic orders, initially from a source size $w_n \approx w_L$ in PM plane down to a spot size $\sigma_n \propto \lambda_n$ at PM focus, yielding large de-magnification factors $\gamma_n \approx w_L/\sigma_n \propto n$ associated to large intensity gains Γ_n at PM focus.

This model is now confronted to 2D PIC simulation results (cf. Fig. 2). Red lines on panels (a)-(b) show that the optimal conditions ($\alpha \leqslant 2$, $w_n/w_L \approx 1$) identified with the model are indeed met for the case of a 3PW laser and a gradient scale length $L = \lambda/8$ originally introduced in Fig. 1. In the proposed scheme where PM curvature is induced by radiation pressure, it was shown that PM denting $\delta_p = 2L\cos^2\theta$ [27]. For the parameters ($\theta = 45^o$,$L = \lambda/8$) used in Figs. 1 and 2, the denting $\delta_p = L$ was $\approx 0.125\lambda$ (corresponding to a radius of

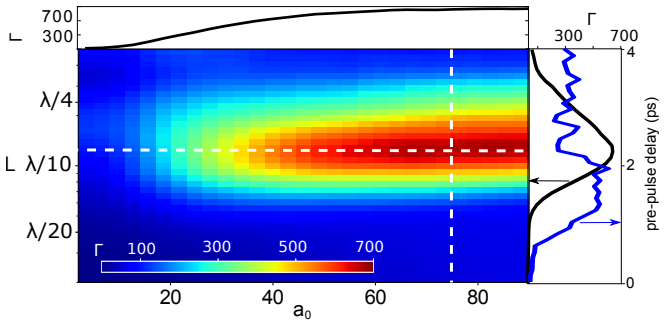

FIG. 3. Intensity gain map of Γ as a function of scale length L and amplitude a_0 for a fixed $\theta = 45^o$ obtained from 2D PIC simulations. The sides panels are a line-outs of the gain map along the white dashed lines. The blue curve represents Γ vs pre-pulse delay τ, with non-isothermal pre-plasma profiles obtained from hydrodynamic simulations (see SM7).

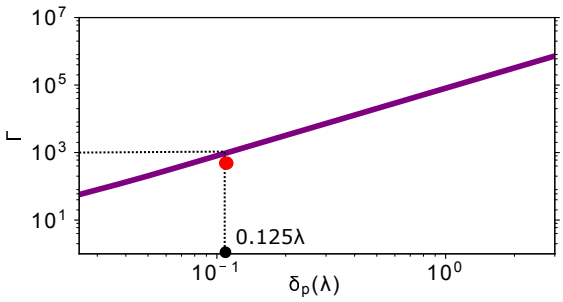

FIG. 4. Evolution of Γ with the PM denting δ_p assuming fixed parameters ($a_0 = 75$, $L = \lambda/8$, $\theta = 45^o$) yielding constant harmonic spectra. The dashed line shows the reference case of $\delta_p = 0.125\lambda$ corresponding to the case of Fig. 1 and 2. Red point: case of the BELLA PW laser (see text).

curvature $R = 2f_p \approx 140\lambda$). Using this value, the harmonic spectrum at PM focus computed from equation (4) (red line on Fig. 2 (c)) is quasi-flat and does not vary with harmonic order. The associated Γ computed from equation (4) predicts ≈ 3 orders of magnitude intensity gains at PM focus in perfect agreement with the results obtained from 3D PIC simulations. This intensity gain mainly comes from the focusing of harmonic orders n such that $\lambda_n < \delta_p$ i.e. $n > 7$ in this case. This means that the laser itself is not focused by the PM and does not contribute to light intensification. This constitutes a huge advantage for probing the QED nature of vacuum, as the reflected laser acts as a "ponderomotive snow-plow" expelling electrons from the focal volume, therefore potentially ensuring a perfect vacuum around harmonic focus (see Fig. 1(a) and SM6).

Note that the proposed scheme expressly requires PW laser power to yield very large intensity gains. Fig. 2 (black lines) indeed shows that the optimal conditions ($\alpha \leqslant 2$, $w_n/w_L \approx 1$) are not met in the TW regime (associated to lower laser amplitudes), which results in much lower intensity gains at PM focus (cf. Fig. 3).

In the proposed scheme where the PM curvature is induced by radiation pressure, δ_p increases with L, which suggests that one could increase Γ indefinitely by augmenting L. However, for too large values of L, recent studies demonstrated that harmonic efficiency can drastically decrease [39, 40], therefore leading to a decrease of Γ. This suggests the existence of an optimal regime that is now determined. As there is currently no model for source sizes and spectrum roll-off (needed in the evaluation of Γ_n) as a function of laser and plasma parameters, the determination of the optimal intensity gain will entirely rely on PIC simulations. To this end, a parameter scan of 1200 $2D$ PIC simulations was run (total of 3 millions core hours, see SM2 [38] for detailed parameters), where a_0 was varied between 2 and 90 and L was varied between $\lambda/50$ and $\lambda/2$ ($\theta = 45^o$ was fixed).

From this extensive set of 2D simulations, the total intensity gain Γ at PM focus was extracted and scaled from 2D to 3D as detailed in SM4-5 [38]. This gain is displayed on Fig. 3, which shows that Γ mainly depends on L for $a_0 > 20$. Indeed, for large enough a_0, harmonic beams are efficiently generated over the laser waist (i.e. $w_n/w_L \approx 1$) resulting in intensity gains Γ_n that scale as $\delta_p^2 \propto L^2$ (cf. equation 4). Starting at low values $L \ll \lambda$, increasing L at first augments δ_p, thus resulting in a rise of Γ as seen on Fig. 3. However, as expected, for larger values of L, harmonic efficiency decreases, eventually leading to a decrease of Γ. This results in the existence of an optimal value of $L \approx \lambda/8$ for $\theta = 45^o$, for which $\Gamma \approx 10^3$ is maximized. These optimal parameters were precisely the ones used in the 3D simulation of Fig. 1. This is the highest intensity gain that can be achieved by employing radiation pressure-induced curvature.

A fascinating prospect would be to keep increasing PM curvature without degrading harmonic properties for approaching intensities close to the Schwinger limit. This could be done by finding techniques that augment δ_p independently of gradient scale length L, as illustrated on Fig. 4 showing the evolution of the total intensity gain Γ with δ_p (computed using eq. (4)) considering fixed interaction conditions (associated to constant harmonic spectra). As suggested by Fig. 4, intensity gains of $\Gamma > 10^5$ (i.e. intensities close to the Schwinger limit for a 3PW laser) could be achieved for $\delta_p > \lambda$ (i.e. radius of curvature $R < 20\lambda$). A possible path to achieve such a control and go beyond the proposed scheme could be to optically structure the initially flat target using spatially shaped pre-pulse beam.

Note that such PM curvature would be extremely difficult to achieve experimentally using pre-engineered solid targets in the form of μm-scale parabolic mirrors [15, 16] instead of optically-structured PMs. Such targets are far beyond present state-of-the-art and would be extremely difficult to align in experiments. Moreover, as opposed to ref. [15] requiring focusing of thousands of harmonic

orders, only ≈ 30 harmonic orders ($7 \leqslant n \leqslant 37$) contribute to Γ in the present scheme, which greatly increases its tolerance to laser and plasma imperfections (see SM7). Plasma imperfections may originate from target defects and non-exponential pre-plasmas. Yet, this scheme uses initially-flat solid targets that can be produced with almost arbitrary low rugosity/planarity. Besides, non-exponential pre-plasma profiles that would be obtained for picoseconds pre-pulse delays in experiments are shown to have negligible effect on the total intensity gain (see blue curve on Fig. 3 right panel and SM7). Finally, it is shown that using the measured laser amplitude and phase profiles of the BELLA PW laser [41] as an input in PIC simulations only results in a tiny decrease of the intensity gain by 38% (see red point on Fig. 4 and SM7) due to laser defects.

To conclude, this letter proposes an all-optical scheme to generate optically-curved PMs from initially flat solid targets that allows reaching intensities beyond $10^{25} W.cm^{-2}$ at PM focus with an incident laser of 3PW. Curvature of the PM in this scheme is achieved by laser radiation pressure and can be controlled by properly tuning the gradient scale length L [27]. Such control has already been demonstrated in experiments employing 100TW lasers [27, 39, 40], suggesting that this scheme could be soon achievable on PW lasers.

The author thanks F. Quéré, G. Bonnaud, J-L Vay and L. Chopineau for precious insights during the writing of the paper. An award of computer time was provided by the INCITE program (Plasm-In-Silico award). This research used resources of the Argonne Leadership Computing Facility, which is a DOE Office of Science User Facility supported under Contract DE-AC02-06CH11357. This work benefited from the support of the project ANR T-ERC PLASM-ON-CHIP of the French National Research Agency (ANR).

* henri.vincenti@cea.fr

[1] D. Strickland and G. Mourou, Optics communications **55**, 447 (1985).
[2] A. Di Piazza, C. Müller, K. Hatsagortsyan, and C. H. Keitel, Reviews of Modern Physics **84**, 1177 (2012).
[3] M. Marklund and P. K. Shukla, Reviews of modern physics **78**, 591 (2006).
[4] A. Bell and J. G. Kirk, Physical review letters **101**, 200403 (2008).
[5] F. Sauter, Zeitschrift für Physik **69**, 742 (1931).
[6] W. Heisenberg and H. Euler, Zeitschrift für Physik **98**, 714 (1936).
[7] J. Schwinger, Physical Review **82**, 664 (1951).
[8] S.-W. Bahk, P. Rousseau, T. Planchon, V. Chvykov, G. Kalintchenko, A. Maksimchuk, G. Mourou, and V. Yanovsky, Optics letters **29**, 2837 (2004).
[9] H. Kiriyama, A. S. Pirozhkov, M. Nishiuchi, Y. Fukuda, K. Ogura, A. Sagisaka, Y. Miyasaka, M. Mori, H. Sakaki, N. P. Dover, K. Kondo, J. K. Koga, T. Z. Esirkepov, M. Kando, and K. Kondo, Opt. Lett. **43**, 2595 (2018).
[10] D. Burke, R. Field, G. Horton-Smith, J. Spencer, D. Walz, S. Berridge, W. Bugg, K. Shmakov, A. Weidemann, C. Bula, *et al.*, Physical Review Letters **79**, 1626 (1997).
[11] J. M. Cole, K. T. Behm, E. Gerstmayr, T. G. Blackburn, J. C. Wood, C. D. Baird, M. J. Duff, C. Harvey, A. Ilderton, A. S. Joglekar, K. Krushelnick, S. Kuschel, M. Marklund, P. McKenna, C. D. Murphy, K. Poder, C. P. Ridgers, G. M. Samarin, G. Sarri, D. R. Symes, A. G. R. Thomas, J. Warwick, M. Zepf, Z. Najmudin, and S. P. D. Mangles, Phys. Rev. X **8**, 011020 (2018).
[12] K. Poder, M. Tamburini, G. Sarri, A. Di Piazza, S. Kuschel, C. Baird, K. Behm, S. Bohlen, J. Cole, D. Corvan, *et al.*, Physical Review X **8**, 031004 (2018).
[13] K. Landecker, Physical Review **86**, 852 (1952).
[14] S. V. Bulanov, T. Esirkepov, and T. Tajima, Physical review letters **91**, 085001 (2003).
[15] S. Gordienko, A. Pukhov, O. Shorokhov, and T. Baeva, Physical review letters **94**, 103903 (2005).
[16] A. A. Gonoskov, A. V. Korzhimanov, A. V. Kim, M. Marklund, and A. M. Sergeev, Physical Review E **84**, 046403 (2011).
[17] N. Naumova, J. Nees, I. Sokolov, B. Hou, and G. Mourou, Physical review letters **92**, 063902 (2004).
[18] A. Solodov, V. Malkin, and N. Fisch, Physics of plasmas **13**, 093102 (2006).
[19] H. C. Kapteyn, M. M. Murnane, A. Szoke, and R. W. Falcone, Optics letters **16**, 490 (1991).
[20] G. Doumy, F. Quéré, O. Gobert, M. Perdrix, P. Martin, P. Audebert, J. Gauthier, J.-P. Geindre, and T. Wittmann, Physical Review E **69**, 026402 (2004).
[21] R. Lichters, J. Meyer-ter Vehn, and A. Pukhov, Physics of Plasmas **3**, 3425 (1996).
[22] T. Baeva, S. Gordienko, and A. Pukhov, Physical review E **74**, 046404 (2006).
[23] B. Dromey, M. Zepf, A. Gopal, K. Lancaster, M. Wei, K. Krushelnick, M. Tatarakis, N. Vakakis, S. Moustaizis, R. Kodama, *et al.*, Nature physics **2**, 456 (2006).
[24] C. Thaury, F. Quéré, J.-P. Geindre, A. Levy, T. Ceccotti, P. Monot, M. Bougeard, F. Réau, P. d Oliveira, P. Audebert, *et al.*, Nature Physics **3**, 424 (2007).
[25] C. Thaury and F. Quéré, Journal of Physics B: Atomic, Molecular and Optical Physics **43**, 213001 (2010).
[26] B. Dromey, D. Adams, R. Hörlein, Y. Nomura, S. Rykovanov, D. Carroll, P. Foster, S. Kar, K. Markey, P. McKenna, *et al.*, Nature Physics **5**, 146 (2009).
[27] H. Vincenti, S. Monchocé, S. Kahaly, G. Bonnaud, P. Martin, and F. Quéré, Nature communications **5**, 3403 (2014).
[28] N. M. Naumova, J. A. Nees, and G. A. Mourou, Physics of plasmas **12**, 056707 (2005).
[29] Y.-J. Gu, O. Klimo, S. V. Bulanov, and S. Weber, Communications Physics **1**, 93 (2018).
[30] G. Blaclard, H. Vincenti, R. Lehe, and J. Vay, Physical Review E **96**, 033305 (2017).
[31] H. Vincenti and J.-L. Vay, Computer Physics Communications **228**, 22 (2018).
[32] J.-L. Vay, I. Haber, and B. B. Godfrey, Journal of Computational Physics **243**, 260 (2013).
[33] H. Vincenti and J.-L. Vay, Computer Physics Communications **200**, 147 (2016).
[34] H. Kallala, J.-L. Vay, and H. Vincenti,

Computer Physics Communications (2019), https://doi.org/10.1016/j.cpc.2019.07.009.
[35] J.-L. Vay, D. Grote, R. Cohen, and A. Friedman, Computational Science & Discovery **5**, 014019 (2012).
[36] `https://picsar.net`.
[37] `http://warp.lbl.gov`.
[38] H. Vincenti, see Supplemental Material (SM), which includes Refs. [42, 43].
[39] S. Kahaly, S. Monchocé, H. Vincenti, T. Dzelzainis, B. Dromey, M. Zepf, P. Martin, and F. Quéré, Phys. Rev. Lett. **110**, 175001 (2013).
[40] L. Chopineau, A. Leblanc, G. Blaclard, A. Denoeud, M. Thévenet, J. Vay, G. Bonnaud, P. Martin, H. Vincenti, and F. Quéré, Physical Review X **9**, 011050 (2019).
[41] A. Jeandet, A. Borot, K. Nakamura, S. W. Jolly, A. J. Gonsalves, C. Tóth, H.-S. Mao, W. P. Leemans, and F. Quéré, Journal of Physics: Photonics **1**, 035001 (2019).
[42] M. Vranic, J. L. Martins, R. A. Fonseca, and L. O. Silva, Computer Physics Communications **204**, 141 (2016).
[43] H. Vincenti, M. Lobet, R. Lehe, R. Sasanka, and J.-L. Vay, Computer Physics Communications **210**, 145 (2017).